The Astrophysical Journal, 767:136 (12pp), 2013 April 20 doi:10.1088/0004-637X/767/2/136

IONIZATION IN ATMOSPHERES OF BROWN DWARFS AND EXTRASOLAR PLANETS. III. BREAKDOWN CONDITIONS FOR MINERAL CLOUDS

Ch. Helling[1], M. Jardine[1], C. Stark[1], and D. Diver[2]
[1] SUPA, School of Physics & Astronomy, University of St. Andrews, St. Andrews KY16 9SS, UK; ch@leap2010.eu
[2] SUPA, School of Physics and Astronomy, University of Glasgow, Glasgow G12 8QQ, UK
Received 2012 July 6; accepted 2013 January 30; published 2013 April 5

ABSTRACT

Electric discharges were detected directly in the cloudy atmospheres of Earth, Jupiter, and Saturn, are debatable for Venus, and indirectly inferred for Neptune and Uranus in our solar system. Sprites (and other types of transient luminous events) have been detected only on Earth, and are theoretically predicted for Jupiter, Saturn, and Venus. Cloud formation is a common phenomenon in ultra-cool atmospheres such as in brown dwarf and extrasolar planetary atmospheres. Cloud particles can be expected to carry considerable charges which may trigger discharge events via small-scale processes between individual cloud particles (intra-cloud discharges) or large-scale processes between clouds (inter-cloud discharges). We investigate electrostatic breakdown characteristics, like critical field strengths and critical charge densities per surface, to demonstrate under which conditions mineral clouds undergo electric discharge events which may trigger or be responsible for sporadic X-ray emission. We apply results from our kinetic dust cloud formation model that is part of the Drift–Phoenix model atmosphere simulations. We present a first investigation of the dependence of the breakdown conditions in brown dwarf and giant gas exoplanets on the local gas-phase chemistry, the effective temperature, and primordial gas-phase metallicity. Our results suggest that different intra-cloud discharge processes dominate at different heights inside mineral clouds: local coronal (point discharges) and small-scale sparks at the bottom region of the cloud where the gas density is high, and flow discharges and large-scale sparks near, and maybe above, the cloud top. The comparison of the thermal degree of ionization and the number density of cloud particles allows us to suggest the efficiency with which discharges will occur in planetary atmospheres.

Key words: astrobiology – brown dwarfs – planets and satellites: atmospheres – plasmas – radiation mechanisms: non-thermal – stars: atmospheres – X-rays: bursts

Online-only material: color figures

1. INTRODUCTION

Electric discharges, including transient luminous events[3] or transient discharges in gases, are non-equilibrium plasmas produced by short-lived electrical conditions of which lightning and associated sprites are the most widely known. Lightning and sprites are commonly observed on Earth. Lightning is also detected or indirectly inferred on most of the cloud-carrying solar system planets. Observations on Earth show that cloud particles or droplets trigger such transient discharges in atmospheric environments (e.g., Yuan et al. 2011). It is not obvious that the underlying physical mechanisms for triggering lightning and sprites are different: they each involve an unbalanced evolution of accelerated free electron populations, driven by electric potential differences. How the latter are created from the organization of ambient gas/particles may be different, but the underlying science is not.

Most of the solar system planets form clouds made of liquids and ices, but depending on local conditions, mineral hazes may also form (e.g., Saunders & Plane 2011). Recent observations of HD 189733b (Pont et al. 2008; Sing et al. 2009, 2011; Gibson et al. 2012) suggest that extraterrestrial giant gas planets contain small mineral dust particles high up in their atmospheres. Further examples include GJ1214b and Kepler 7b.

Prompted by the abundance of discharge processes in clouds on Earth and in the clouds of solar system planets, we take a first look at the conditions for such discharge events in extrasolar, planetary, and brown dwarf atmospheres. The essential requirements are the presence of both an electric field (electric potential difference) and free electrons. This electric field accelerates the free electrons through the ambient gas. If they collide with other gas particles sufficiently frequently and with enough energy to liberate increasingly more electrons, an electron avalanche is produced. The critical electric field required for this depends, to some extent, on the composition of the gas. This avalanche can develop into a self-propagating ionization front (streamer) if the self-field of the electrons in the avalanche is similar to the strength of the applied external field. If the avalanche has reached a critical size, then it can propagate into areas with a lower electric field strength in which an avalanche would not start normally. Two electrical breakdown mechanisms are known to occur in dielectrics: the conventional breakdown occurring, for example, in glow discharges; and the runaway breakdown which is suggested to play a role in lightning discharges on Earth. The threshold electric field needed to initiate the avalanche of a runaway breakdown appears one order of magnitude below that for a conventional breakdown (for more details see Roussel-Dupre et al. 2008; Marshall et al. 1995). Each of the resulting streamers is a highly conducting plasma channel in which the density of non-thermal electrons is greatly increased and from which electrons leak into the ambient gas.

Helling et al. (2011) have argued that dust clouds that are made of mineral particles can be charged, e.g., by gas turbulence induced dust–dust collisions. The cloud particles remain charged for long enough that discharge events can occur

[3] In the community of terrestrial atmospheric physics, the term *transient luminous event* is used to describe sprites, elves, and blue-jets only, but not lightning.

and streamers can be established. Other possible processes for charge separation, which we have not considered, are, e.g., different contact potentials of the material making up the grain, and fractoemission or collisional charging of polarized grains in an external electric field (Pähtz et al. 2010). The Coulomb recombination time of cloud particles by thermal electrons is long enough that electric fields can establish between passing grains which then can initiate subsequent electron avalanche processes leading to streamers (Figure 4 in Helling et al. 2011). The result is that during the electron avalanche phase, there is an exponential increase in free charges for each free electron that exists in the gas phase. Numerical experiments that simulate an avalanche from the initial electron up to and beyond the avalanche-to-streamer transition demonstrate consistently that a single electron seeding a streamer can cause the occurrence of 10^{12}–10^{13} secondary non-thermal electrons for a certain time interval (Dowds et al. 2003; Ebert et al. 2010).

Laboratory studies suggest that during grain–grain impact, smaller grains are more negatively charged compared to larger grains of the same composition (Lacks & Levandovsky 2007; Forward et al. 2009; Merrison et al. 2012). A similar conclusion was reached from volcano ash experiments (Hatakeyama & Uchikawa 1952; Kikuchi & Endoh 1982; James et al. 2000). Experimental results for different minerals are not available at present. Experiments on wind-driven entrainment of Martian dust (mainly iron oxides) and Basalt dust (Na/K/Ca-silicates) by Merrison et al. (2012) suggest average electric charge values of $10^3, \ldots, 10^5\ e^-\ \mathrm{grain}^{-1}$. The exact values might, however, be influenced by the experimental set-up (Aplin et al. 2012). These experiments were carried out under pressures between 10 mbar and 1 bar. Only a very weak pressure dependence on the number of charges per grain was seen. No strong dependence on the grain material was found either, but one order of magnitude variation is suggested due to grain sizes, morphology, and abundance of grains. They found no evidence for a dependence of dust electrification on atmospheric composition.

The extrasolar atmospheric environments we are looking at in brown dwarfs and giant gas planets have local temperatures between $T_{\rm gas} = 500$ K–4000 K and gas pressures between $p_{\rm gas} \approx 10^{-10}$ bar–10 bar. This pressure range comprises the pressure interval for Mars-dust analog experiments by Merrison et al. (2012). The resulting degree of ionization by thermal processes in brown dwarfs and giant gas planet atmospheres is $\chi_{\rm e} = p_{\rm e}/p_{\rm gas} \approx 10^{-15}$ to 10^{-7} throughout the atmosphere, which is very low (Helling et al. 2012), but enough to start an electron avalanche. The formation of dust by seed formation and bulk growth takes place in a temperature window of ∼500–2100 K and leads to the formation of mineral clouds. Gravitational settling, convective mixing, and element depletion are major associated processes. Helling et al. (2008c) have shown that the upper cloud (i.e., low temperature and low-pressure) will be dominated by small, dirty (i.e., inclusions of other materials) silicate grains with inclusions of iron and metal oxides, and the warmer, denser cloud base by bigger, dirty iron grains with metal inclusions. The actual size of the cloud particles deviate from this mean value according to a height dependent size distribution (Figure 8 in Helling et al. 2008c). The chemical composition of the grains as well as their size distribution change with height inside a cloud in a quasi-stationary environment.

The different scale regimes involved in the formation of atmospheric clouds suggest the consideration of two different scale regimes with respect to charge and discharge processes. The large scale regime is where the cloud particles settle gravitationally (rain out) according to their mass and size, or where they are transported by hydrodynamical processes like convection. This will leave the smallest and potentially more negatively charged particles suspended in the higher layers, while the larger and more positively charged particles populate the lower part of the cloud. The small scale regime describes the scales at which cloud particles interact during grain–grain collisions, where colliding particles (droplet) or individual cloud particles produce point discharges (also called *corona*) that may start large-scale lightning. This analogy is drawn from the discharge experiments for Earth conditions where colliding drops in storms and ice particles can produce point discharges which are thought to be able to initiate lightning (for more details see MacGorman & Rust 1998). A similar scenario is suggested in Merrison et al. (2012), and was utilized by Farrell et al. (1999) and Michael et al. (2008) to model Martian dust storms.

What are the conditions to trigger a discharge event which subsequently increases the local density of free electrons by non-thermal processes potentially leading to the occurrence of lightning or associated transient luminous events like sprites? The local electric field, E, must exceed the ionization threshold of the ambient gas, hence a critical field strength, $E_{\rm crit}$, and seed electrons for the development of an electron avalanche need to be present. We note that measurements of the actual threshold electric field strength for a terrestrial lightning flash in a cloud are not easy to obtain (Marshall et al. 2005). Marshall et al. (1995) performed balloon experiments from which they derived electric breakdown thresholds that led them to hypothesize that lightning flashes might be initiated by runaway breakdown. This paper therefore presents a first investigation of the discharge behavior in extrasolar atmospheres by studying the following questions.

1. What electric field strength is needed to allow breakdown phenomena known from Earth and solar system planets to occur in extrasolar, planetary objects and brown dwarfs?
2. What can we learn about the breakdown conditions in extrasolar objects, for example breakdown distances, minimum voltages, or chemistry dependence?
3. What are the critical conditions for breakdown such as cloud size, grain size, and number of charges per surface? Under which conditions can the critical field strength be produced by grains alone?
4. How many thermal electrons are available in a mineral cloud of a brown dwarf or a giant gas planet in order to trigger a streamer event? How efficiently can discharge events occur, and hence influence the gas phase composition?

To answer these questions, we first outline the basic ideas and relations for an electrostatic breakdown in gases of different chemical compositions in Section 2. These relations are evaluated in Section 3 for previously calculated model atmosphere structures of brown dwarfs and giant gas planets. We are using Drift-Phoenix model atmosphere structures that are the result of the solution of the coupled equations of radiative transfer, convective energy transport (modeled by mixing length theory), chemical equilibrium (modeled by laws of mass action), hydrostatic equilibrium, and dust cloud formation (Dehn 2007; Helling et al. 2008a, 2008b; Witte et al. 2009; Witte et al. 2011). The dust cloud formation model includes a model for seed formation (nucleation), surface growth, and evaporation of mixed materials. The effects of gravitational settling (drift) and convective overshooting on the cloud formation are explicitly included

in our dust model equations (Woitke & Helling 2003, 2004; Helling & Woitke 2006; Helling et al. 2008c). The results of the Drift-Phoenix model atmosphere simulations include, for example, the gas temperature–pressure structure ($T_{\rm gas}, p_{\rm gas}$), the local gas-phase composition, the local electron number density ($n_{\rm e}$), the number of dust grains ($n_{\rm d}$), and their height dependent sizes (a). These models are determined by the effective temperature, $T_{\rm eff}$ (K), the surface gravity, g (cm s^{-2}), and the initial element abundances, which are set to the solar values unless specified otherwise. The final element abundances are determined by element depletion due to dust formation. We also discuss how many charges per surface would be needed to initiate a field breakdown based on this model output (Section 3.2), and we estimate the enrichment rate of the gas phase by streamer electrons (Section 3.4). Section 4 contains our conclusions.

2. BREAKDOWN CHARACTERISTICS

Electric breakdown is the process of transforming a non-conducting substance into a conductor as the result of applying a sufficiently large electric field. This ionization state of the bulk gas phase builds up over times between $10^{-8}, \ldots, 10^{-4}$ s and is large enough that it is accompanied by a light flash. A gas-phase breakdown is a threshold process, and hence it occurs when the local electric field exceeds a value characteristic of the special local conditions.

A streamer develops in the wake of a positively charged tail of a primary avalanche during which an accelerated electron travels through an ambient gas. If the energy of the accelerated electron exceeds the ionization potential of the gas, then the growth of a thin ionization channel (streamer) between two electrodes results. These electrodes can be capacitor plates, charge distributions inside clouds, or grains. The transition between an avalanche process and the streamer mechanisms is not well documented so far. Raether (1964) suggests that the streamer mechanism dominates at an electrode distance of 5–6 cm, the exact value of which might change depending on local conditions.

The onset of electric field breakdowns has been studied for charge distributions on capacitor plates for a variety of gases and characteristic quantities, and the breakdown voltage has been parameterized for easy use based on lab experiments (Equations (1) and (2); e.g., Raizer 1991). Different electric field strengths inside a capacitor were tested for different gases. For practical reasons, the parameterization of the breakdown voltage has only been done for terrestrial or solar system gas mixtures or for homogeneous gases, which may not resemble the gas composition in an extrasolar planetary or brown dwarf atmosphere.

The resulting Paschen curve, which relates the breakdown voltage with the product pd (Equation (1), Figure 1), shows that the breakdown voltage of a capacitor, $V_{\rm t}$ [V], depends only on the material of the cathodes (characterized by Townsend's second ionization coefficient γ), the gas between the capacitor plates (characterized by the coefficients A (cm^{-1} torr^{-1}) and B (V cm^{-1} torr^{-1})), and the product between the gas pressure and the capacitor plate separation, pd (cm torr),

$$V_{\rm t} = \frac{B \cdot pd}{C + \ln(pd)} \quad \text{with} \quad C = \ln \frac{A}{\ln\left(\frac{1}{\gamma} + 1\right)} \tag{1}$$

$$\frac{E_{\rm t}}{p} = \frac{B}{C + \ln(pd)}. \tag{2}$$

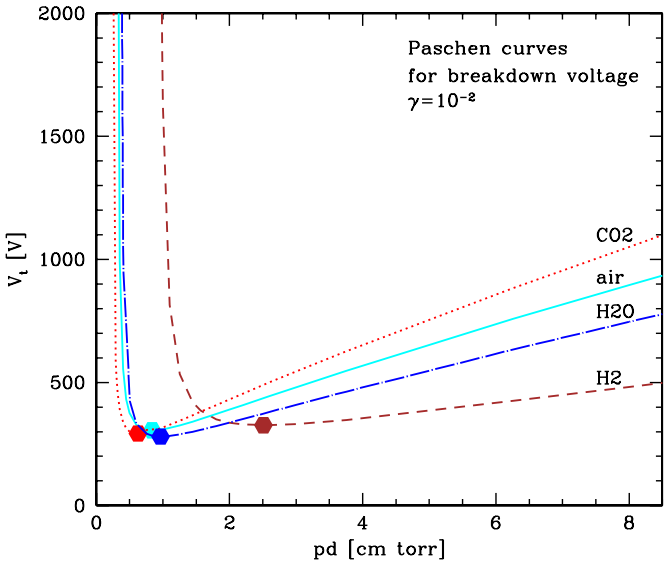

Figure 1. The Paschen curve shows the dependence of the breakdown voltage, $V_{\rm t}$ [V] on the product of gas pressure, p, and the minimum breakdown distance, d, for four molecular gases composed of H_2, H_2O, CO_2, and of air. The classical Paschen curve depicted here, has a minimum (indicated by the symbol; Stoletow point) which we use to determine the minimum electric breakdown field in brown dwarf and exoplanetary atmospheres in Figures 2 and 3.

(A color version of this figure is available in the online journal.)

Townsend's second ionization coefficient γ is the effective secondary emission coefficient of the cathode and can be calculated as the ratio between the number of electrons ejected per incident ion. We will refrain from doing so and apply numbers given in the literature. γ varies between 10^{-9} for organic cathode materials and 10^{-2} for nickel and copper cathodes (Table 4.10 in Raizer 1991). If $\gamma = 1$, then there is one ionization event per hit. However, the breakdown voltage becomes independent of the cathode material when a spark breakdown or a streamer starts to develop. This is evident from the fact that lightning on Earth is not triggered by electron emission of the cloud "cathodes," the negatively charged part of a cloud.

Qualitatively, the Paschen curve predicts that the breakdown voltage decreases as the electrode gap decreases because the corresponding electric field increases. The Paschen curve proved to be accurate for large gaps and low pressures but it is observed to fail at extremely low and high pd-values. We note that experiments show that the Paschen curve is not necessarily accurate in describing breakdowns between electrode spaces of less than 15 μm. Go & Pohlman (2010) have therefore derived a model for a modified Paschen curve for breakdown in micro-scale gaps. In their model, the breakdown voltage does not have a singularity ($+\infty$) for small gap sizes, but instead decreases further (see their Figure 1). The observation that $pd = $ const does not hold for small gaps, and p and d become independent variables. For the small-scale cases considered, i.e., the distance between two charge centers in the form of grains, the gap size is just large enough to allow us to apply the classical Paschen curve formalism (Figure 2).

At some gap size, the classical Paschen curve has a minimum, the Stoletow point, which is calculated from $dV_{\rm t}/d(pd) = 0$, resulting in

$$pd = \frac{e}{A} \ln\left(\frac{1}{\gamma} + 1\right). \tag{3}$$

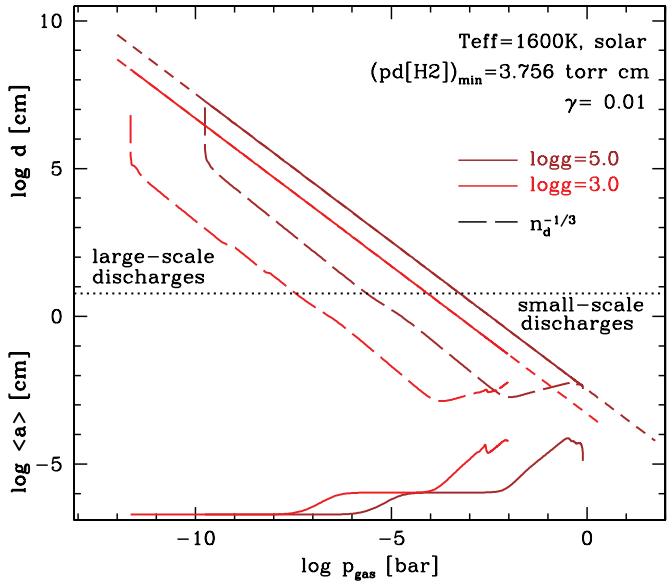

Figure 2. The minimum separation of charges of two capacitor plates (representing our charge carrying surfaces like on clouds or on grains) required for discharge (solid and short-dashed in the upper part of the plot). The distance d corresponds to the Paschen minimum where $p_{\rm gas} \cdot d = 2.509$ torr cm (=5007 dyn cm^{-2} cm) for an H_2 gas. Note, an artificial offset between the $\log(g) = 5.0$ (brown, "log $g = 5.0$") and the $\log(g) = 3.0$ (red, "log $g = 3.0$") was applied; all curves should lie on top of each other without this offset. $p_{\rm gas} \cdot d$ is a constant for a given A (cm^{-1} torr^{-1}) and γ, hence, the same for all atmospheres of the same chemical composition. In this plot, an H_2 gas is assumed for which $A[H_2] = 5$ cm^{-1} Torr^{-1} (Raizer 1991) and Townsend's second ionization coefficient $\gamma = 0.001$ is used. The solid lines show the pressure interval where clouds form and the dashed lines show the whole atmospheric pressure range modeled. Raizer (1991) notes that discharge sparks set in if the plate distance is >6 cm (horizontal dotted line) which helps us here to distinguish between large-scale and small-scale discharges. We overplot two more length scales for comparison: The dust–dust mean free path $n_{\rm d}^{-1/3}$ (long dashed lines) and the mean grain sizes, $\langle a \rangle$, at the bottom of the plot.

(A color version of this figure is available in the online journal.)

pd is a local constant for a given gas composition (expressed by the constants A, B) and for a given capacitor surface material (expressed by the Townsend's second ionization coefficient γ) as long as the gap d is large enough. The product pd will therefore be the same for any planet or brown dwarf, given that they have the same gas composition. The capacitor plate distance, d, which in our small-scale case is the distance between passing grains, changes with the local gas pressure, which in our case is a proxy for the vertical position in the atmosphere (Figure 2).

Figure 1 shows $V_{\rm t}(pd)$ with the Stoletow point of these gas-chemistry-dependent Paschen curves indicated by octaeder symbols. Brown dwarfs would be best represented by the Paschen curve for H_2 (brown dashed line) and giant gas planets will very likely exhibit a more complex gas-phase composition because they form from a protoplanetary disk at different distances from the host stars therein. The minimum breakdown voltage $V_{\rm t,min}$ (V) follows by inserting Equation (3) into Equation (1) (left),

$$V_{\rm t,min}(pd) = \frac{e^1 B}{A} \ln\left(\frac{1}{\gamma} + 1\right). \quad (4)$$

Thus, for each gas composition, there is a minimum voltage required to achieve electric breakdown in the gas. Only then can a streamer or subsequent lightning develop. It may, however, be more useful to express this condition in terms of the electric field strength $\boldsymbol{E}$. With $E = |\boldsymbol{E}| = |-\partial\phi(r)/\partial r|$, and $\phi(r)$ the electric potential and voltage $V = \Delta\phi(r)$ being the potential difference (Δ) between two points (hence, the units are the same), it follows that $E = V/r$ for a spherical charge distribution at a radial distance r from the charge Q ($E = V/d$ for a capacitor). Inserting Equation (3) into Equation (2), the breakdown or ignition field strength follows with $E = |-\partial\phi/\partial r|$ from the following relation:

$$\frac{E_{\rm t,min}}{p} = B \quad \Rightarrow \quad E_{\rm t,min} = Bp. \quad (5)$$

Hence, $(E_{\rm t,min}/p) =$ const is a universal constant of a gas in the capacitor or the gas exposed to the electric field of some charge distribution. $E_{\rm t,min}$ is the minimum electric field strength needed to achieve breakdown. Raizer (1991) and Sentman (2004) have published $(E_{\rm t,min}/p)$-values for various gases and gas mixtures potentially representative of the solar system planetary atmospheres. These values are based on either experiments or calculations that take into account details of the interaction processes of the electron with the ambient gas. For example, Sentman (2004; brought to our attention by Y. Yair 2008, private communication) deals with gas mixtures by Boltzman modeling of the electron distribution function for a given gas composition (added to Table 1). Hence, details on the acceleration process, scattering, and energy losses/gains are "hidden" in the measured material constant. A detailed review of a kinetic approach can be found in Roussel-Dupre et al. (2008). We summarize the values in Table 1 as some of the original literature is hard to come by. For more details on composition dependencies, consult Chapter 6 in Meek & Craggs (1978).

In summary, once the gas composition is defined for a given brown dwarf or gas giant planet, the pressure variation with height defines the variation of the minimum electric field needed for breakdown in the atmosphere, which we will investigate in more detail below.

3. RESULTS

The breakdown quantities introduced in the previous section will now be evaluated for a set of atmosphere structures that were previously calculated using the Drift-Phoenix model atmosphere code by Witte et al. (2009). These model atmospheres provide the required input quantities for the following calculations, which are the local gas pressure, $p_{\rm gas}$, and grain sizes, a, for each height in the atmosphere. Two models are studied in detail: $T_{\rm eff} = 1600$ K, $\log(g) = 5.0$ as the example for a brown dwarf atmosphere, and $T_{\rm eff} = 1600$ K, $\log(g) = 3.0$ as the example for a non-irradiated giant gas planet. Both atmospheres have an initially solar metallicity. Later in the paper, we compare these results to models of different effective temperature $T_{\rm eff} = 1600, 1900, 2100, 2500$ K and 2800 K (Figure 8), and the initial metallicity is varied between $[M/H] = -5, \ldots, 0$, with $[M/H] = 0$ indicating the solar values (Figure 9). The comparison among these models allows us to identify trends in the electric breakdown quantities in substellar and low-metallicity atmospheres.

3.1. Classical Breakdown Quantities

Breakdown distance, d. Assuming that a charge separation has built up in a brown dwarf or planetary atmosphere, how far can two imaginary capacitor plates be apart that a breakdown of the atmospheric gas will occur for an established electric field?

Table 1
Parameterization of Electric Breakdown Field According to Paschen Curves: Material Constants A & B Taken from Raizer (1991) and from Sentman (2004), pd and $V_{t,min}$ Calculated from Equations (3) and (4)

	A (1/(cm Torr)) (Raizer 1991)	B (V/(cm Torr)) (Raizer 1991)	pd_{min} (cm Torr) (This Paper)	$V_{t,min}$ (V) (This Paper)
He	3	34	4.181	142.2
H_2	5	130	2.509	326.1
N_2	12	342	1.045	357.5
Air	15	365	0.8363	305.2
CO_2	20	466	0.6272	292.3
H_2O	13	290	0.9649	279.8
Sentman (2004)	A (1/(cm Torr))	$E/p = B$ (V/(cm Torr))	pd_{min} (cm Torr)	$V_{t,min}$ (V)
Venus ($CO_2/N_2 = 96.5/3.5$)	7.27	180	2.58	465
Earth ($N_2/O_2/Ar = 78/21/1$)	7.44	243	2.53	617
Mars ($CO_2/N_2/Ar = 95.5/2.8/1.7$)	7.23	178	2.60	462
Jupiter ($H_2/He/CH_4 = 89/10.9/0.1$)	6.19	143	3.06	434
Saturn ($H_2/He/CH_4 = 96.3/3.6/0.1$)	7.46	156	2.52	392
Titan & Tritan ($N_2/CH_4 = 95/5$)	8.80	274	2.13	585
Uranus ($H_2/He/CH_4 = 82.5/15.2/2.3$)	6.47	138	2.90	401
Neptune ($H_2/He/CH_4 = 80/18.5/1.5$)	622	135	3.02	408

This is the distance of two capacitor plates, or two otherwise charge-carrying surfaces, that can build up an electric field between them, as described by the Paschen minimum where $p_{gas} \cdot d = 2.509$ torr cm (=5007 dyn cm^{-2}) for an H_2 gas (Equation (3), Figure 1). This is the distance where the electrical breakdown would be easiest according to Equation (4). Hence, for $p_{gas} \cdot d$ below the Paschen minimum, the breakdown voltage increases sharply in the classical case. However, Go & Pohlman (2010) show that lower breakdown voltages should be expected at smaller distances, justifying our use of the classical Paschen curve as a first step to study breakdown characteristics. $p_{gas} \cdot d$ is a constant for a given A (cm^{-1} torr^{-1}) and γ, and hence is the same for all atmospheres of the same chemical composition with respect to the most abundant gas-phase species. This allows us to calculate the breakdown distance d for a known p_{gas}-structure of a model atmosphere.

Figure 2 shows the breakdown distance as a function of the local gas pressure calculated for the pressure structure of a brown dwarf ($T_{eff} = 1600$ K, $\log(g) = 5.0$, solar element abundances, brown line) and a giant gas planet ($T_{eff} = 1600$ K, $\log(g) = 3.0$, solar element abundances, red lines) assuming that molecular hydrogen ($A[H_2] = 5$ cm^{-1} Torr^{-1}; Raizer 1991) is the dominant gas species to be ionized by electrons accelerated in the electric field. This assumption is appropriate as H_2 is the most abundant molecule in the atmosphere models applied here. The assumption breaks down if H_2 ionizes in the hot and dense inner layers of the atmosphere where clouds cannot be thermally stable, and where atomic hydrogen is the dominating gas component. The Townsend's second ionization coefficient $\gamma = 0.001$ is used, representing a conducting cathode material that is strictly correct only for $T > 1800$ K from which iron dominates the grain material composition in the cloud. As mentioned earlier, it is only relevant to consider the material dependence of γ for the avalanche process, not so for the streamer.

Figure 2 shows that the breakdown distance varies over the atmosphere pressure ranges from $\sim 5\,\mu$m in the densest regions to 10^5 Km in the upper, low-pressure regions (dashed lines). This suggests that discharges could appear spatially extended and diffuse in low-pressure regions, while numerous discharge events remain small, locally confined phenomena in high-pressure regions. It also suggests that different electric discharge processes dominate at different heights: local corona (point discharges) and small-scale sparks at the bottom of the cloud, and glow discharge and large-scale sparks at the top.

In a quasi-static environment, these different processes could lead to a neutralization of large-scale charge build-up and consequently diminish the possibility for a large-scale lightning. However, hydrodynamic atmosphere motions are driven by convection and by gravity waves (Freytag et al. 2010) on brown dwarfs which are also rapid rotators (Scholz et al. 2011). This suggests that large-scale charge separation is likely to be sustained by convection-like processes comparable to Earth, for example, like in the Hadley cells at Earth's equator.

Following the observation in Raizer (1991) that for breakdown distances $>5, \ldots, 6$ cm the streamer mechanism will dominate and sparks can develop, we distinguish a large-scale ($d > 6$ cm) and a small-scale regime ($d < 6$ cm) in Figure 2.

It is interesting to compare the maximum spacial separation that can exist between two charge distributions while still permitting a discharge, to the average size of the cloud particles and their mean particle distance. For simplicity, we consider the altitude dependent mean grain size $\langle a \rangle$ instead of separate grain size distributions for each altitude as shown in Helling et al. (2008c). The mean grain size, $\langle a \rangle$, is always smaller than the maximum distance, d, over the whole geometrical extension of the cloud. The mean distance between the cloud particles scales with the cloud particle number density as $n_d^{-1/3}$. Consequently, it will be largest where the number density is smallest. The "knee" at the high-pressure end of each long-dashed curve in Figure 2 corresponds to the maximum cloud particle number density (compare the upper panel in Figure 10). Generally, the cloud particles have a mean separation that is $\sim$3.5 orders of magnitude smaller than the maximum break-through distance in a giant gas planet cloud ($\sim$2.5 for the brown dwarf cloud). This comparison also shows that the cloud particles have considerable separation in the upper cloud region, suggesting that collective phenomena such as large-scale charge distributions are to be

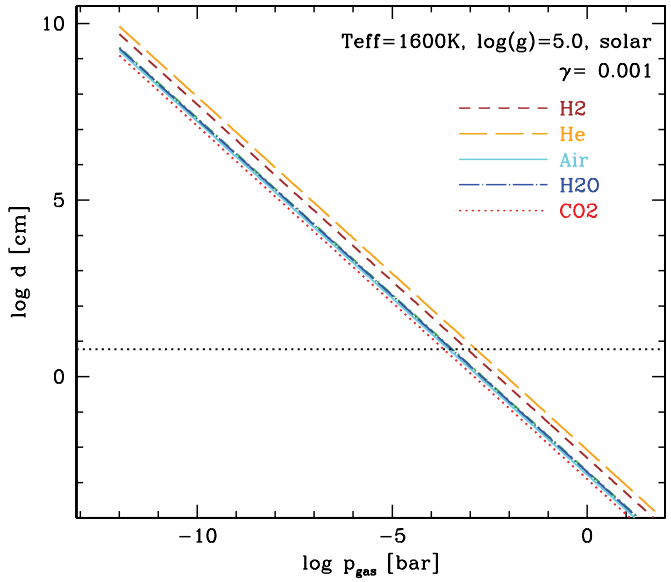

Figure 3. Dependence of breakdown distance d at the Stoletow point on the composition of the ionized gas. The variation in these distances for six cases (H_2, He, air, H_2O, CO_2; Table 4.1 in Raizer 1991) shows that the uncertainty resulting from atmospheric composition is a factor of 10. This estimate also covers differences in A depending on the pressure regime in which the measurements were made (high (∼1 bar) vs. low pressure; Table 7.1 in Raizer 1991). Sentman (2004) has published data for mixed gases but the lack of a consistent notation makes application difficult.

(A color version of this figure is available in the online journal.)

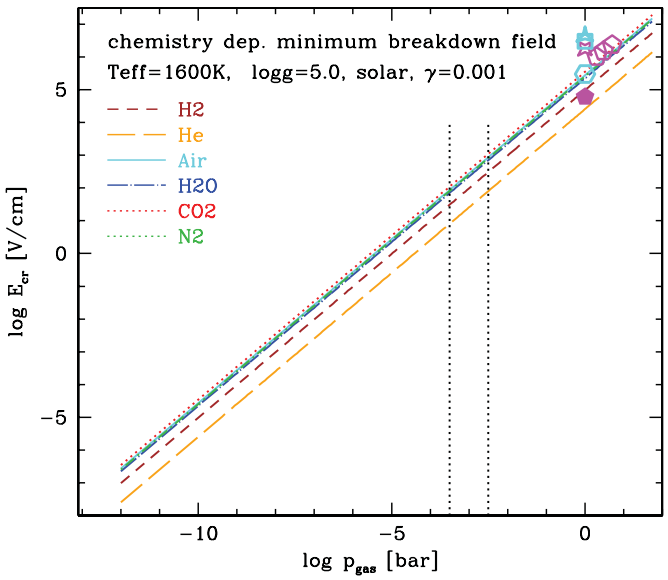

Figure 4. The minimum critical breakdown electric field corresponding to the minimum of the Paschen curve for individual ionized gases (H_2, He, air, H_2O, CO_2; Table 4.1 in Raizer 1991). Pressures higher than indicated by the vertical dotted line correspond to $d < 6$ cm, and pressures lower than indicated by the vertical dotted line correspond to $d > 6$ cm according to Figure 3. (This set of dotted double lines results from the intersection interval of the dotted line in Figure 3.) The symbols indicate the breakdown field for Earth (cyan) and Jupiter (magenta) as given in Yair et al. (1995, Table 1; open symbols: measured; solid: with drops and ice; stars: theoretical estimate).

(A color version of this figure is available in the online journal.)

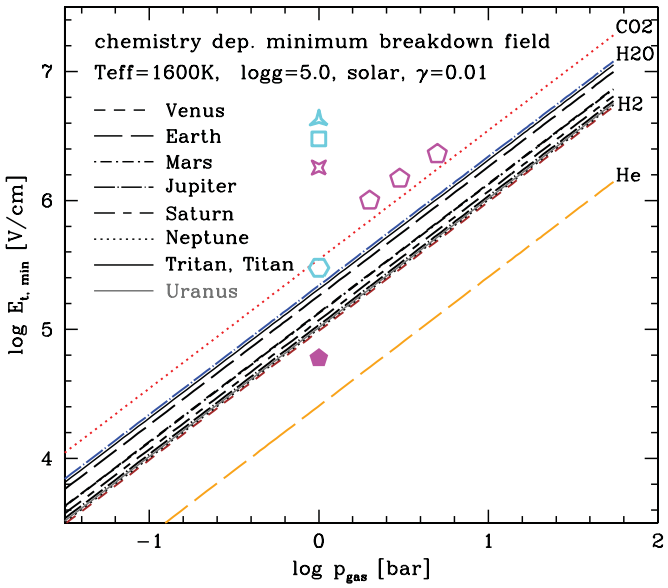

Figure 5. The minimum critical breakdown electric field for a brown dwarf atmosphere with $T_{\rm eff} = 1600$ K and $\log(g) = 5.0$ assuming that the field break down happens in different gas compositions. This is a zoom into Figure 4 for CO_2 (red dotted), H_2O (blue long-dashed), H_2 (brown dashed), and He (orange long dashed), with the curves assuming the solar system planetary atmosphere compositions overplotted in black. The curve for Uranus and Neptune lie almost on top of each other.

(A color version of this figure is available in the online journal.)

expected rather than inter-particle discharges such as in the high-pressure part of the cloud. However, if the breakdown distance is smaller than the maximum value d (e.g., in a turbulent flow), small-scale discharge processes may also occur in the low-pressure part of an atmosphere.

Note that the mean particle size and the cloud particle number density are determined by the processes of dust and cloud formation (nucleation, growth/evaporation, drift, convective mixing, element depletion) which are taken into account in the DRIFT-PHOENIX model atmospheres. Coagulation, for instance, could change the grain size distribution, but it is not clear a priori how it changes since a variety of constructive and destructive collisional processes occur (Güttler et al. 2010). Furthermore, turbulence (Helling et al. 2001, 2004) and gravity waves (Freytag et al. 2010) cause local, hydrodynamic density increases, neither of which is taken into account in the present paper.

Depending on the ionizing gas, these global values of d have uncertainties of one order of magnitude, as we demonstrate for different gas-phase compositions in Figure 3. The breakdown distances inside the cloud regions (solid lines, Figure 2) are somewhat different in a brown dwarf mineral cloud and in a giant planet's mineral cloud because the brown dwarf clouds exist at higher pressures. The exact values of discharge quantities, such as the maximum separation of charge distributions before breakdown but also the required number of charges, will therefore differ between objects of different effective temperature, surface gravity, and metallicity (see Figures 8 and 9).

Minimum electric field for breakdown $E_{\rm t,min}$. The minimum electric field strength needed for a gas breakdown scales with the local gas pressure (Equation (5)), as is shown in Figure 4. This critical breakdown field strength corresponds to the minimum of the Paschen curve for individual ionized gases (H_2, He, air, H_2O, CO_2; Table 4.1 in Raizer 1991), represented by individual parameters B (V cm^{-1} torr^{-1}) and a given Townsend's second ionization coefficient $\gamma = 0.001$. The results are shown for a sample model atmosphere ($T_{\rm eff} = 1600$ K, $\log(g) = 5$, initial solar composition) for which we vary the parameter B to show the dependence on gas composition. Figure 4 shows the results for pure gases (data from Raizer 1991) and Figure 5 for mixed

gases of the solar system planets (data from Sentman 2004). Overplotted in Figure 4 are the values given in Yair et al. (1995: magenta, Jupiter cloud with drops and ice; cyan, Earth values; full symbol, Paschen formula; open symbols, measurements). This shows that the values are comparable. The vertical lines in Figure 4 indicate the large-scale regime (low pressure) and the small-scale regime (high pressure) for pressures corresponding to Figure 3.

The minimum critical breakdown field strength varies between 10^7 V cm^{-1} at high atmospheric pressures and 10^{-7} V cm^{-1} in low pressure regions where $p_{\rm gas} = 10^{-12}$ bar. The breakdown fields on Earth (at sea level) and on Jupiter are $\sim 10^4 \ldots 10^6$ V cm^{-1}, which correspond to the values at 1 bar in Figures 4 and 5. The dependence on the local gas composition introduces an uncertainty of one order of magnitude as demonstrated in Figure 4.

Figure 5 shows a close-up of Figure 4 showing the minimum breakdown field using the data for the different solar system planets in comparison with the two most different examples of gas phase composition (CO_2 and He gas). The results for the solar system planets sit between a pure H_2O (upper limit) and a pure H_2 atmosphere (lower limit).

We further note that values measured for the onset of coronal discharges on a treeless plot of grass are about 3 orders of magnitude lower (40 V cm^{-1}; MacGorman & Rust 1998) than the respective value at 1 bar in Figures 4 and 5. MacGorman & Rust (1998) also point out that point discharges from ice crystals that are dominated by their surface (rather than bulk) conductivity seem likely in thunderstorms for a field strength >400 kV m^{-1} (4×10^3 V cm^{-1}), which is still $\sim$2 orders of magnitude lower than the classical values in Figures 4 and 5.

Therefore, our results suggest that electrical breakdown can readily occur in cloudy atmospheres of brown dwarfs and giant gas planets.

3.2. How Many Charges are Needed for an Electric Field Breakdown?

Laboratory measurements of grain charges suggest that single grains can carry 10^3–10^5 e grain^{-1}. This is supported by experiments on photoelectrical charging of dust in a vacuum (Sickafoose et al. 2000; metals and glass), grain levitation (Fortov et al. 2001), measurements of grauple on Earth (Lamb & Verlinde 2011), and wind-driven entrainment of Martian dust (Merrison et al. 2012; silicates and iron oxide). Somewhat higher charge loads are suggested from dust–dust collision experiments (e.g., contact electrification and tribo-electrification) with silicate granules by Poppe et al. (2000) resulting in 10^{-5} C m^{-2} (i.e., $\sim 5 \times 10^6$ e grain^{-1} for $a = 1.2$ μm), and by volcanic ash experiments involving dust charging by fractoemission by James et al. (2000) resulting in 10^{-8} to $10^{-6.5}$ C m^{-2} ($\sim 10^5$ to $10^{7.5}$ e cm^{-2}). How do these experimental numbers compare to the number of charges needed to initiate a field breakdown in a substellar atmosphere?

The minimum electric field strength that needs to be overcome in order to produce a field breakdown in an astrophysical gas with a low degree of ionization (see Figure 10, upper panel, solid lines) varies only by one order of magnitude between gases of different molecular composition for a given gas pressure. Furthermore, the breakdown voltage measured above thunderclouds on Earth is up to two order of magnitude lower than the classical breakdown values that were discussed here so far (see also the discussion at the end of Section 3.1). Keeping these uncertainties in mind, we continue with studying how many charges are needed to initiate a field breakdown in a gas of a given composition for the minimum breakdown voltage $V_{\rm t,min}$.

The assumption of a spherically symmetric charge distribution (Equation (6)) allows a first order-of-magnitude study, although neither clouds nor cloud particles are truly spherical. Equation (6) is a general expression which allows us to distinguish between these two scale regimes of clouds and grains later on. With the radial distance from a charge distribution of $Q_{\rm crit}$ charges set to the minimum distance for breakdown, d, it follows that

$$Q_{\rm crit} = 4\pi\epsilon_0\, d\, V_{\rm t,min}\ ({\rm C}) \Rightarrow Q_{\rm crit} \propto d \propto \frac{1}{p[{\rm Pa}]}. \qquad (6)$$

One electron carries only a tiny fraction of a Coulomb: 1 C = $6.24150965\,10^{18}$ e. The surface charge density for a charge distribution of radius r (grain radius or cloud radius) is given by $\sigma = Q/(4\pi r^2)$. Thus, the critical surface charge density for breakdown is

$$\sigma_{\rm crit} = \frac{\epsilon_0\, d\, V_{\rm t,min}}{r^2} = \epsilon_0 E_{\rm r,min}\left(\frac{d}{r}\right)^2 \quad ({\rm C\,cm^{-2}}) \qquad (7)$$

($\epsilon_0 = 8.85\,10^{-12}$ F m^{-1}[4]—vacuum dielectric constant or electric permittivity of free space). Note that the proportionality at the right hand side of Equation (6) *only holds if* the radial distance from the charge distribution is set to the minimum distance for breakdown according to the minimum of the Paschen curve (Equation (3)). Note also that the pressure needs to be in SI units (Pa) for $Q_{\rm crit}$ to be in units of elementary charges on the right hand side of Equation (6).

The charge carrying surface, $4\pi r^2$, of our charge distribution can be the effective surface of a cloud or the surface of a single grain ($r = a$). The total charge carrying surface of the cloud, the effective cloud surface, will be provided by the total surface of the particles that form the cloud, rather than being related to the geometrical cloud radius. On large vertical scales, the cloud particles will settle depending on their masses and sizes. Our stationary cloud formation model suggests a large mean grain size at the lower edge of the clouds and a small mean grain size in the cloud's top region (Woitke & Helling 2004; Witte et al. 2009). Smaller particles will remain suspended for longer in the atmosphere than the more positively charged bigger grains. On small scales, the charge separation needed to build up an electric field is influenced by non-spherical grain shapes and chemical surface inhomogeneities, neither of which is included in our considerations yet. For spheroidal grain growth, we refer to Diver & Clarke (1996) and Stark et al. (2006).

Our cloud formation model (Woitke & Helling 2003, 2004; Helling & Woitke 2006; Helling et al. 2008c) allows us to link numerically derived cloud properties, like grain sizes, grain number densities, and dust surface, to critical breakdown quantities as evaluated in the previous sections. The solution of our cloud model in the frame of the radiative transfer code Phoenix (Hauschildt & Baron 1999) allows us to link dust properties and the critical breakdown quantities to the atmospheric temperature and pressure scale of a brown dwarf or giant gas planet as result of the Drift-Phoenix model atmosphere simulations (Dehn 2007; Helling et al. 2008a, 2008b; Witte et al. 2009).

The moment equations of our kinetic dust formation model (Gail & Sedlmayr 1988; Dominik et al. 1993; Woitke & Helling 2003) allow us to calculate the total dust surface available per

[4] ϵ_0 is in SI unites F m^{-1} with F = As/V (A: Ampere) = C/V (C Coulomb) = C^2/(N m).

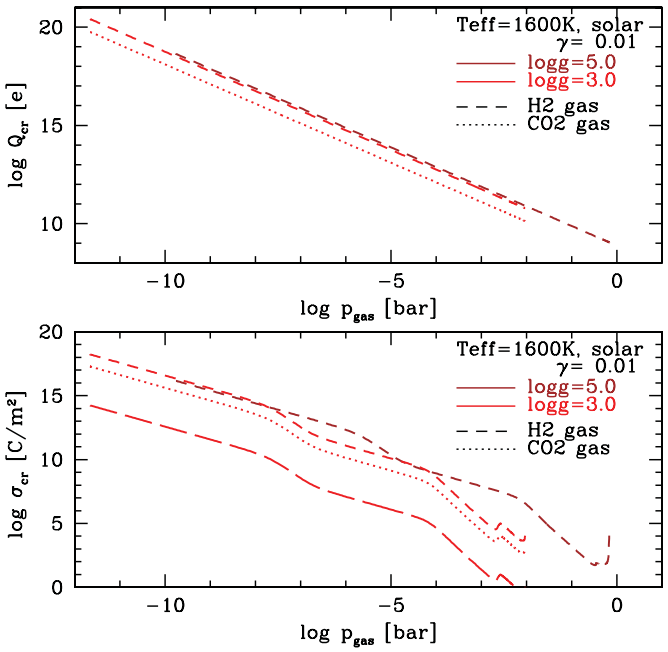

Figure 6. Top: the total number of charges needed to overcome the breakdown field (Equation (6)) for an H_2 dominated gas in a mineral cloud in a brown dwarf atmosphere (brown) and a giant gas planet (red). These charges are assumed to exist on two charge-carrying surfaces separated by the minimum distance for discharge. The case of a CO_2-dominated atmosphere is overplotted for the giant-gas planet (dotted line). Bottom: the critical surface charge density, $\sigma_{\rm cr} = Q_{\rm cr}/(4\pi r^2)$, critical for an electric field breakdown. $\sigma_{\rm cr}$ was calculated for $r = \langle a(T, \rho_{\rm gas})\rangle$ assuming that all grains are of the size of the local mean grain size, except for the long-dashed line which shows $\sigma_{\rm cr}$ for $100 \times \langle a\rangle$. Note that $1\ {\rm C\,m^{-2}} = 6.24 \times 10^{14}\ e\ {\rm cm^{-2}}$.

(A color version of this figure is available in the online journal.)

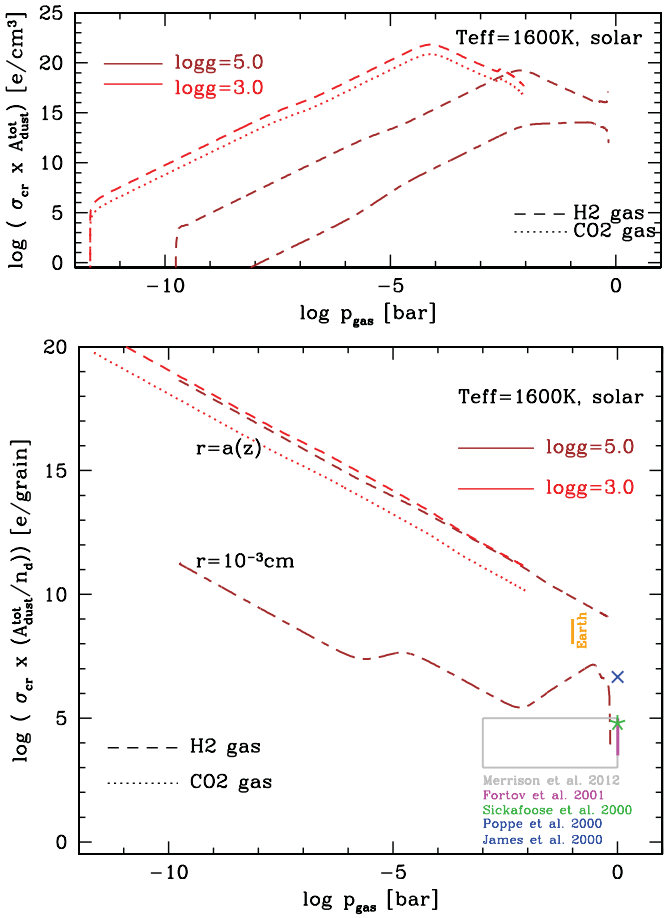

Figure 7. Critical number of charges needed for electric breakdown in mineral clouds inside atmospheres for objects with $T_{\rm eff} = 1600$ K, and $\log(g) = 3.0$ (red) and $\log(g) = 5.0$ (brown). Upper panel: the charges on the total dust surface $A^{\rm tot}_{\rm dust}$ per cm^3 of atmospheric gas as $\sigma_{\rm cr} \times A^{\rm tot}_{\rm dust}$ (e cm^{-3}). Lower panel: the number of charges per dust grain $\sigma_{\rm cr} \times (A^{\rm tot}_{\rm dust}/n_{\rm d})$ (e grain^{-1}). The symbols represent the following data sources: gray rectangle, Merrison et al. (2012); magenta vertical bar, Fortov et al. (2001); green asterisk, Sickafoose et al. (2000); blue cross, Poppe et al. (2000) and James et al. (2000); orange vertical bar, values for Earth hale from Lamb & Verlinde (2011).

(A color version of this figure is available in the online journal.)

unit volume ($A^{\rm tot}_{\rm dust}$), and also the mean surface of a grain ($\langle A_{\rm dust}\rangle$) depending on atmospheric height (i.e., depending on the local temperature and pressure),

$$A^{\rm tot}_{\rm dust} = \sqrt[3]{36\pi}\, L_2 \quad ({\rm cm^2\ cm^{-3}}) \tag{8}$$

$$\langle A_{\rm dust}\rangle = \sqrt[3]{36\pi}\, L_2/L_0 = A^{\rm tot}_{\rm dust}/n_d \quad ({\rm cm^2}). \tag{9}$$

L_0 is the zeroth and L_2 the second moment of the grain size distribution function, respectively (e.g., Helling et al. 2001). Equations (8) and (9) allow us to relate the total number of charges needed for breakdown to the total grain surface per unit volume (upper panel, Figure 7) and to the numbers of grains (lower panel, Figure 7) available as follows:

$$\sigma \times A^{\rm tot}_{\rm dust}\ [e^-\ {\rm cm^{-3}}]\ : \text{number of charges per total dust surface per gas volume} \tag{10}$$

$$\sigma \times \frac{A^{\rm tot}_{\rm dust}}{n_d}\ [e^-\ {\rm grain^{-1}}]\ : \text{number of charges per grain.} \tag{11}$$

Note that the total dust surface, i.e., the total cloud particle surface, is related to the charge carrying surface inside a cloud.

The number of charges required to establish an electric field large enough for a breakdown to occur and subsequently ionize the ambient gas depends on the local gas pressure. More charges are needed in the low density (pressure) regime of an atmosphere, for example, as Figure 6 demonstrates, because of the large maximum breakdown distance (compare Figures 2 and 3). The lowest density layers would require a total of about 10^{20} charges to allow an electron avalanche with a subsequent streamer to develop. The actual number depends to a certain extent on the dominating gas species that is being ionized, as in the example for H_2O and CO_2 in Figure 6. The lower panel of Figure 6 presents this results in (SI) units of critical charge density, $\sigma_{\rm crit}$ [(C cm^{-2}), assuming that the charges would be located on the grains of the size of the local mean grain size, hence $r = \langle a(T, \rho_{\rm gas})\rangle$. Artificially increasing the radius of the charge carrying surface to $r = 100 \times \langle a(T, \rho_{\rm gas})\rangle$ (long dashed red line) verifies the anticipated result of a decreasing critical charge density with increasing surface area that would allow an electric field breakdown.

Figure 7 (upper panel) shows the critical number of charges, $\sigma_{\rm crit} \times A^{\rm tot}_{\rm dust}$ (e^- cm^{-3}), as distributed over the total dust surface per cm^3 of atmospheric gas depending on altitude (represented by the local atmospheric gas pressure). The dust surface is provided by a large number of large dust grains at higher pressure and by a small number of smaller grains at lower pressures at the cloud top. If the same total dust surface would be provided by grains of a constant size of 10^{-3} cm (brown

long-dash short dash line), then the critical number of charges per cm^3 would decrease by more than five orders of magnitude.

The lower panel of Figure 7 shows the critical number of charges per grain, $\sigma_{\rm crit} \times (A^{\rm tot}_{\rm dust}/n_d)$ [e^- grain^{-1}], which takes into account the total dust surface and the number of grains present throughout the cloud. Each grain has to carry considerably less charge at the bottom of the cloud compared to the cloud top as more grains are available here. Due to gravitational settling, most of the grains are contained in the deeper cloud where the number of grains is much higher than at the cloud top.

Our results suggest that many charges per grain are required to initiate a breakdown discharge in the upper part of the clouds in brown dwarfs and giant gas planets. Such a height-dependent charge distribution results because we apply our results for the maximum breakdown distance, d, which is rather large at the cloud top as demonstrated in Figures 2 and 3. The breakdown distance can, however, decrease by, e.g., turbulent or other non-local wind processes which are not taken into account here. A decreasing number of charges needed to initiate an electric field breakdown would then result. Additionally, the charge density, σ, depends on the radius of the charge carrying surface, r. Therefore, we again assess our results for r larger than $\langle a \rangle$, but now by using a constant grain size of 10^{-3} cm (brown long-dash short dash line) throughout the cloud. The comparison with the experiments with mono-disperse grain ensembles as performed by Sickafoose et al. (2000; green star in Figure 7), Fortov et al. (2001; magenta vertical bar in Figure 7), Merrison et al. (2012; blue box in Figure 7), Poppe et al. (2000; blue asterisk in Figure 7), James et al. (2000; blue asterisk in Figure 7), and values for grauple on Earth from Lamb & Verlinde (2011; orange vertical bar in Figure 7) suggest that our results for mineral clouds are not unreasonable, especially if we allow that cloud particle sizes can be larger than the mean grain size from our dust model. Such a deviation from the mean grain size is to be expected as our study of the grain size distribution in Helling et al. (2008c) demonstrates. Furthermore, the critical breakdown field strengths applied here are upper values as suggested by experiments on Earth thunderstorms and can, hence, be expected to be one to two orders of magnitude lower with the corresponding decreasing effect on the necessary number of charges. The chemical richness of the mineral clouds in the atmosphere of brown dwarfs and giant gas planets may introduce further uncertainties compared to the laboratory experiments cited above. The actual material composition may influence the charge distribution on the grain surface leading, for example, to further polarization effects of the cloud particles. The question of how many charges a dust grain can carry before it is destroyed by the electrostatic stress will be addressed in a forthcoming paper.

Trends with $T_{\rm eff}$ and metallicity [M/H]. The quantities that determine if the streamer mechanism occurs and with what efficiency it does so are determined by the local gas pressure because the gas pressure determines the mean free path of the seed electrons inside the gas of brown dwarfs and planets in the electric field. Global quantities that determine an atmosphere's pressure structure are the effective temperature, $T_{\rm eff}$, the metallicity, $[M/H]$, and the surface gravity, $\log(g)$, of the object, in the case of non-irradiated objects. The influence of the surface gravity has already been shown in Figures 6 and 7. We use the surface gravity to distinguish between brown dwarfs ($\log(g) = 5.0$) and giant gas planets ($\log(g) = 3.0$).

Figures 8 and 9 show the influence of $T_{\rm eff}$ and $[M/H]$, respectively, for a small number of Drift-Phoenix models. The

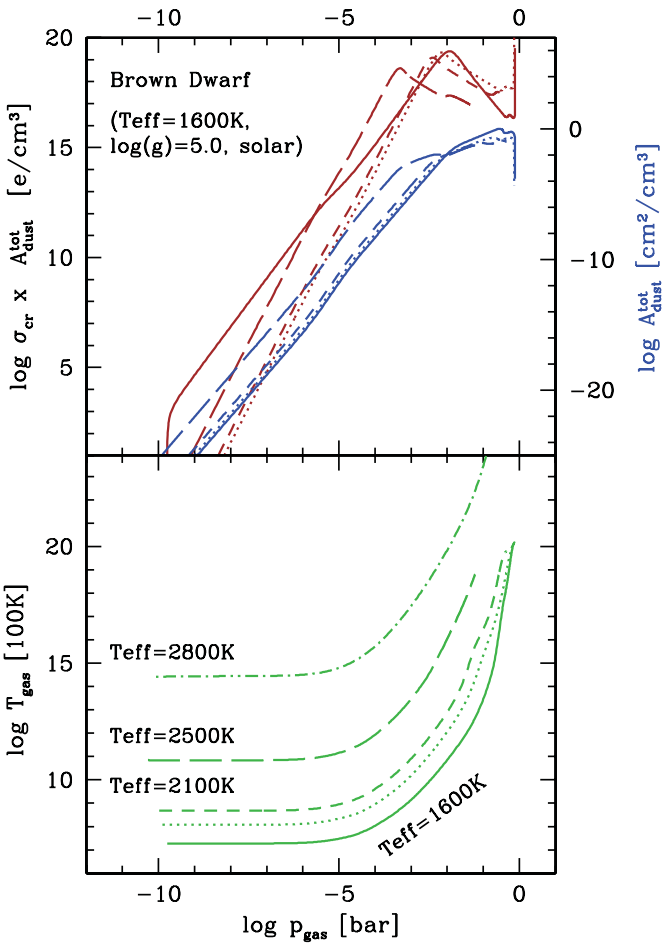

Figure 8. Critical charge number density, $\sigma_{\rm cr}$ (e cm^{-3}) per total dust surface needed to overcome the local breakdown field depending on the effective temperature of the object (top panel). The results are plotted for five solar-metallicity brown dwarf model atmospheres ($\log(g) = 5.0$) with $T_{\rm eff} = 1600$ K (solid), 1900 K (dotted), 2100 K (short dashed), 2500 K (long dashed), 2800 K (dash-dotted). The lower panel (local gas temperature) demonstrates why the critical surface charge density $\sigma_{\rm cr}(p)$ changes for different effective temperatures.

(A color version of this figure is available in the online journal.)

metallicity $[M/H]$ is given relative to the solar abundances, and hence $[M/H] = -3.0$ stands for the initial element abundances being decreased by 10^{-3} compared to the solar values. The lowest panels in both figures demonstrate how the Drift-Phoenix temperature–pressure profiles change with changing metallicity. The local pressure mainly increases for a given local temperature for an increasing $T_{\rm eff}$ (Figure 8), while the upper atmospheric parts of the ($T_{\rm gas}$, $p_{\rm gas}$)-structures stay relatively comparable with decreasing metallicity for given $T_{\rm eff}$ and $\log(g)$. The inner atmospheric regions, however, show an increasing gas pressure with decreasing metallicity for a given gas temperature.

The critical charge number density needed to initiate the occurrence of streamers that subsequently might lead to lightning does change by up to four orders of magnitude for a given gas pressure among the models of varying effective temperature that form dust clouds. Note that the $T_{\rm eff} = 2800$ K model in Figure 8 is too hot for dust condensation processes to be efficient. The metallicity of the atmospheric gas has a larger impact on the local temperature. Figure 9 shows that the critical charge number density can differ in the low-metallicity cases much more than

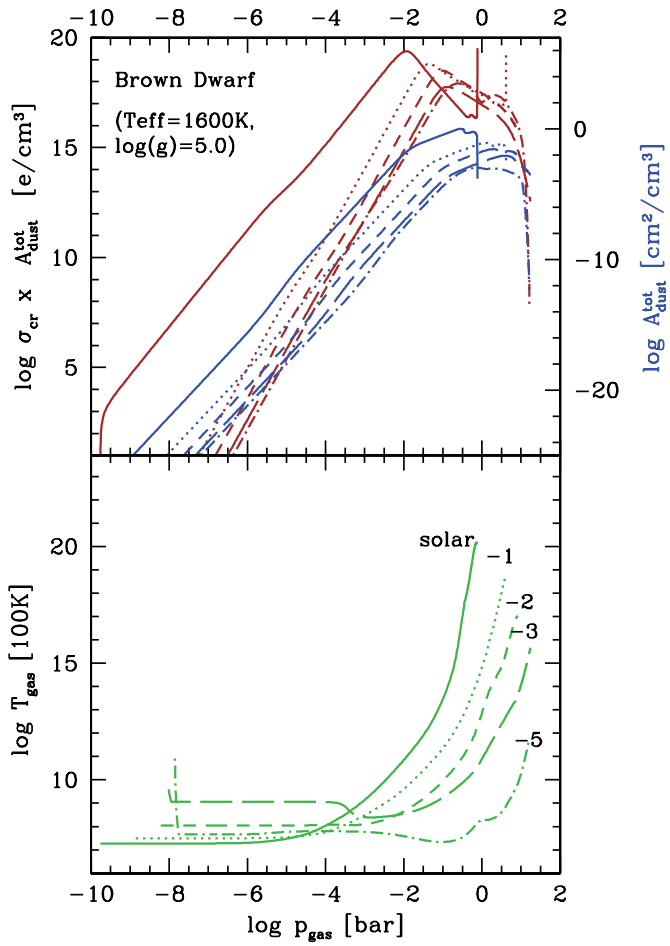

Figure 9. Critical charge number density, $\sigma_{\rm cr}$ (e cm^{-3}) per total dust surface, needed to overcome the local breakdown field depending on the metallicity of the object (top panel). The results are plotted for five brown dwarf model atmospheres ($\log(g) = 5.0$) with different metallicities $[M/H] = 0$ (solar, solid), -1 (dotted), -1 (short dashed), -3 (long dashed), -5 (dash-dotted). The lower panel (local gas temperature) demonstrate why the critical surface charge density $\sigma_{\rm cr}(p)$ changes for different $[M/H]$.

(A color version of this figure is available in the online journal.)

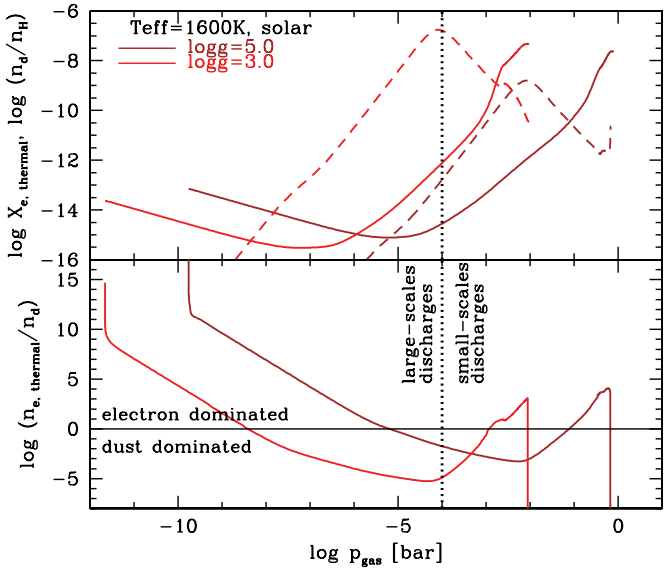

Figure 10. Efficiency of discharges in planetary atmospheres with mineral clouds. Top: degree of thermal gas ionization, $\chi_{\rm e,thermal} = n_{\rm e}/n_{\rm H}$ (solid lines), and the dust number density per hydrogen, $n_{\rm d}/n_{\rm H}$ (dashed lines), for a brown dwarf and a giant gas planet atmosphere for the same Drift-Phoenix models as in Figure 6. Bottom: the ratio of the number of thermal electrons, $n_{\rm e,thermal}$, to the number of cloud particles, $n_{\rm d}$, provides a measure of the efficiency with which a streamer may be initiated in a mineral cloud. Two different regimes appear: above the black line—electron dominated, hence more than one electron is available per grain pair, below the black line—dust dominated, hence less than one electron is available per grain pair. The dotted vertical lines distinguished the cloud regimes of potential large-scale cloud discharges and small-scale, inter-grain discharges similar to Figures 2–4.

(A color version of this figure is available in the online journal.)

for varying $T_{\rm eff}$. Note that the dust surface available to host the charges does vary among the models, with the largest differences again occurring for changing metallicities in the lowest metallicity cases (dashed/dotted line) compared to the solar case (solid line). All models, however, exhibit a comparable total dust surface in the inner, denser regions at the bottom of the cloud. Witte et al. (2009) demonstrated that low-metallicity atmospheres can produce larger dust grains at the inner edge of the cloud than in the solar case if $[M/H] > = -4.0$.

3.3. Number of Electrons versus Number of Grains

So far, we have studied the breakdown conditions utilizing classical arguments and laboratory measurements assuming that the gaseous atmosphere would have enough free electrons available to start the electric breakdown process. However, is the number of thermal electrons large enough in brown dwarf and giant gas planet atmospheres to provide the seed electrons that are needed to start an electron avalanche in the electric field, for example between two passing grains? The investigation of this question allows us to estimate the efficiency with which streamer discharges could occur inside brown dwarf and giant gas planet atmospheres. Streamer discharges are the starting point for large-scale phenomena like lightning that may be followed by a sprite into the less dense atmosphere above.

We compare the degree of thermal ionization, $\chi_{\rm e,thermal} = n_{\rm e,thermal}/n_{\rm H}$ (solid lines), with the number of dust grains per hydrogen, $n_{\rm d}/n_{\rm H}$ (dashed lines), in Figure 10 (top panel), and we use these two quantities to estimate an efficiency of streamer initiation in a mineral cloud by calculating the ratio $n_{\rm e,thermal}/n_{\rm d}$ (Figure 10, bottom panel). Hence, this efficiency would be the number of streamers per grain pair if each of the thermal electrons in the electric field of two charged grains would initiate an electron avalanche. In the previous section, we evaluated the conditions under which such a field breakdown can occur.

Figure 10 shows that the efficiency, $n_{\rm e,thermal}/n_{\rm d}$, varies with height, as at some height the dust number density can have a local maximum while the number of thermal electrons is a rather smooth function of gas pressure which is linked to the gas temperature by the underlying atmosphere model. Hence, the number of electrons available for each colliding pair of charge-carrying grains decreases as shown in the lower panel of Figure 10. Here, more than one electron would be available to initiate the avalanche process for all pressures above the solid black, horizontal lines ($n_{\rm e,thermal} = n_{\rm d}$), and less than one electron would be available below this line. In both cases, for the brown dwarf atmosphere (brown) and the giant gas planet's atmosphere (red), the efficiency of streamer initiation would vary between 1 and $\approx 10^{-5}$. $n_{\rm e,thermal}/n_{\rm d} = 1$ means that one streamer per grain pair sets off, and $n_{\rm e,thermal} < n_{\rm d}$ means that not every grain pair can initiate a streamer event. To generalize, we can distinguish two regimes regarding the streamer efficiency in a cloud forming atmosphere, the occurrence of which can be

less homogeneous if the whole grain size distributions for each atmospheric layer are taken into account

$$\begin{array}{lll} n_{\rm e,thermal} > n_{\rm d} & \text{electron-dominated} & n_{\rm e,thermal}/n_{\rm d} \gg 1 \\ n_{\rm e,thermal} < n_{\rm d} & \text{dust-dominated} & n_{\rm e,thermal}/n_{\rm d} \leqslant 1,\ \ldots,\ 10^{-5}. \end{array}$$

The consequence is that the discharge process in cloudy atmospheres will be determined by two populations, the population of the cloud particles and the population of free electrons, respectively. Both populations need to be abundant enough to allow discharge processes to develop into streamers as the precondition for the occurrence of lightning.

3.4. An Estimate of Electron Enrichment of the Gas Phase by Dust–Dust-induced Streamer Events in Mineral Clouds

The empirical formula

$$\alpha = A\,p\exp\left(\frac{-Bp}{E}\right) \quad \Rightarrow \quad \alpha(E_{\rm min}) = \frac{Ap}{e} \tag{12}$$

for Townsend's ionization coefficient, α ($\rm cm^{-1}$), enables us to provide first estimates of the number of electrons created when an electron avalanche starts that might develop into a streamer. Streamers are discussed as a likely possibility to initiate lightning (see Section 5.4 in MacGorman & Rust 1998). α is the number of ionization events performed by an electron in a 1 cm path along an electric field. This interpretation is only true if we assume that the electron undergoes ionization collisions only for high values of E/p and moderate electron energies (Raizer 1991). The constants A and B are the same constant given in Table 1 for approximating experimental curves. αd would then be an estimate for the number of electrons produced if the electron avalanche would stretch along the whole critical breakdown distance d (compare Figure 2). The total number of non-thermal electrons per unit time, $N_e^{\rm aval}(\rm s^{-1})$, produced by all possible seed electrons that lead to an electron avalanche can be approximated by

$$N_{\rm e}^{\rm aval} \approx f_{\rm eff} \times \alpha d \times \nu_{\rm coll}^{\rm dd}(z) \tag{13}$$

$$\approx \frac{n_{\rm e,thermal}}{1/2 \cdot n_{\rm d}} \times \alpha d \times \nu_{\rm coll}^{\rm dd}(z), \tag{14}$$

with $\nu_{\rm coll}^{\rm dd}(z)$ being the frequency of dust–dust collisions at each height z in the atmosphere as derived in Equation (17) in Helling et al. (2011). Following from Section 3.3, we define $f_{\rm eff} = n_{\rm e,thermal}/(1/2 \cdot n_{\rm d})$ which provides an estimate of the efficiency with which an avalanche could occur. $f_{\rm eff} > 1$ suggests a superposition of avalanches that are each started by one gas-phase electron.

An electron avalanche can turn into a self-propagating ionization front by the subsequent development of a streamer in its positively charged wake. This instability can trigger much larger plasma-channel structures like sprites above thunderclouds or lightning bolts below and inside a cloud which we are not considering for our estimate here. The elementary streamer alone, however, results in a number of local non-thermal electrons much larger than predicted by the classical Townsend breakdown by electron avalanche (Equation (12)). Numerical experiments suggest the production of $10^{12}, \ldots, 10^{13}$ electrons per streamer event (e.g., Dowds et al. 2003). Multiple streamers develop if more than one electron is "seen" by a pair of charged grains or two otherwise oppositely charged charge distributions.

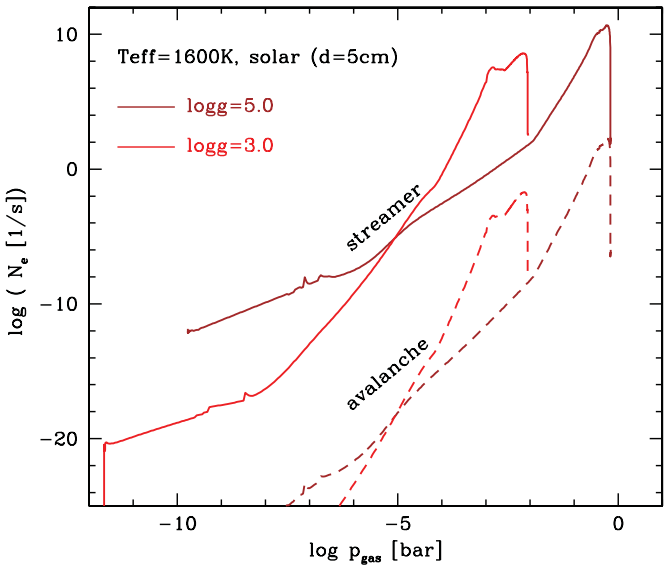

Figure 11. Gas-phase enrichment by dust–dust collision triggered discharges. Electron avalanche (dashed lines; $d = 5$ cm used) yields considerably less free charges than streamer events (solid lines). The same brown dwarf (brown) and a giant gas planet (red) atmosphere models are used as in Figure 10.

(A color version of this figure is available in the online journal.)

This efficiency depends on the number of free electrons that are already present in the gas before a streamer-triggering electron avalanche develops, and has been derived in Section 3.3. For a streamer breakdown, the number of non-thermal electrons produced during a collisional approach of two dust particles that occur with the frequency $\nu_{\rm coll}^{\rm dd}(z)$,

$$N_{\rm e}^{\rm streamer} = \frac{n_{\rm e,thermal}}{1/2 \cdot n_{\rm d}} \times 10^{12} \times \nu_{\rm coll}^{\rm dd}(z). \tag{15}$$

Given the different nature of an electron avalanche and a streamer, the electron production occurs with a different efficiency. The result is that $N_{\rm e}^{\rm streamer} \gg N_{\rm e}^{\rm aval}$ (Figure 11). Our results in Figure 11 further suggest that the largest impact of the streamer electrons on the local chemistry could be expected in the inner, denser cloud regions in brown dwarfs and giant gas planets.

4. CONCLUSIONS

The discharge process requires (1) charge separation on cloud particles and (2) a charge separation over large distances to allow large-scale discharges such as lightning or sprites to occur. The laboratory experiments (Poppe et al. 2000; James et al. 2000; Fortov et al. 2001; Lacks & Levandovsky 2007; Forward et al. 2009; Merrison et al. 2012) for a variety of minerals (including Martian and volcanic minerals), for graupel on Earth (Lamb & Verlinde 2011), as well as our own investigations (Helling et al. 2011) suggest that mineral cloud particles will be charged. Mineral cloud particles settle gravitationally in brown dwarfs and giant gas planets such that a large scale charge separation can occur inside these clouds. Convection serves as an additional large-scale charge separation mechanism. If small grains are indeed more negatively charged than large grains as suggested by experiments (Hatakeyama & Uchikawa 1952; Kikuchi & Endoh 1982; James et al. 2000; Merrison et al. 2012), then spatial charge separation will occur on a large scale by gravitational settling but also on small scales by particle size effects alone. Our investigations of the minimum

distance that two charge distributions need to have for a electric field breakdown to occur (Figure 2) suggest that small-scale discharges should be expected in high-pressure regions of an atmospheric cloud. Large-scale discharge processes should occur in the upper, low-pressure part of the cloud. This is consistent with observations from Earth where, for example, sprites develop into the low-pressure part of the atmosphere above a thunder-cloud event.

The critical electric field strength to be overcome for a field breakdown varies between 10^7 V cm^{-1} at high atmospheric pressures and 10^{-7} V cm^{-1} in the upper atmosphere where the gas pressure is low. The critical number of charges per total dust surface per cm^3 change from 10^{23} e cm^{-3} in the inner atmosphere to $<10^5$ e cm^{-3} in the low pressure atmosphere. These numbers compare well with experimental values at the 1 bar pressure level. The number of charges needed to initiate the occurrence of streamers that subsequently might lead to lightning does not change substantially among the atmosphere models of varying effective temperature that form dust clouds. The critical number of charges has the same trend in the low-metallicity cases as for varying effective temperatures.

Generally, a population of charged cloud particles and enough free electrons are needed to allow transient luminous events to occur in extraterrestrial, cloudy atmospheres. The ratio of both determines the efficiency with which discharge events may occur. The rate of electron enrichment is highest in the high-pressure part of the cloud as here, according to our model, a larger charge-carrying surface is available. This is where we expect small-scale discharges to dominate.

We highlight financial support of the European Community under the FP7 by an ERC starting grant. Y. Yair is thanked for providing Sentman (2004). Ch.H. acknowledges the hospitality of the University of Vienna during the beginning of the paper's work. Most literature search was performed using the ADS. Our local computer support is highly acknowledged.

REFERENCES

Aplin, K. L., Goodman, T., Herpoldt, K. L., & Davis, C. J. 2012, P&SS, 69, 100
Dehn, M. 2007, PhD thesis, Univ. Hamburg
Diver, D. A., & Clarke, D. 1996, JPhD, 29, 687
Dominik, C., Sedlmayr, E., & Gail, H.-P. 1993, A&A, 277, 578
Dowds, B. J. P., Barrett, R. K., & Diver, D. A. 2003, PhRvE, 68, 026412
Ebert, U., Nijdam, S., Li, C., et al. 2010, JGR, 115, A00E43
Farrell, W. M., Kaiser, M. L., Desch, M. D., et al. 1999, JGR, 104, 3795
Fortov, V. E., Nefedov, A. P., Molotkov, V. I., Poustylnik, M. Y., & Torchinsky, V. M. 2001, PhRvL, 87, 205002
Forward, K. M., Lacks, D. J., & Sankaran, R. M. 2009, GeoRL, 36, 13201
Freytag, B., Allard, F., Ludwig, H.-G., Homeier, D., & Steffen, M. 2010, A&A, 513, 19
Gail, H.-P., & Sedlmayr, E. 1988, A&A, 206, 153
Gibson, N. P., Aigrain, S., Pont, F., et al. 2013, MNRAS, 428, 3680
Go, D. B., & Pohlman, D. A. 2010, JAP, 107, 103303
Güttler, C., Blum, J., Zsom, A., Ormel, C. W., & Dullemond, C. P. 2010, A&A, 513, 56
Hatakeyama, H., & Uchikawa, K. 1952, PMG, 2, 85
Hauschildt, P. H., & Baron, E. 1999, JCoAM, 109, 41
Helling, Ch., Dehn, M., Woitke, P., & Hauschildt, P. H. 2008a, ApJL, 675, L105
Helling, Ch., Dehn, M., Woitke, P., & Hauschildt, P. H. 2008b, ApJL, 677, L157
Helling, Ch., Jardine, M., Diver, D., & Witte, S. 2012, P&SS, in press
Helling, Ch., Jardine, M., & Mokler, F. 2011, ApJ, 737, 38
Helling, Ch., Klein, R., Woitke, P., Nowak, U., & Sedlmayr, E. 2004, A&A, 423, 657
Helling, Ch., Oevermann, M., Lüttke, M. J. H., Klein, R., & Sedlmayr, E. 2001, A&A, 376, 194
Helling, Ch., & Woitke, P. 2006, A&A, 455, 325
Helling, Ch., Woitke, P., & Thi, W.-F. 2008c, A&A, 485, 547
James, M. R., Lane, S. J., & Gilbert, J. S. 2000, JGR, 105, 16641
Kikuchi, K., & Endoh, T. 1982, J. Meteorol. Soc. Jpn., 60, 548
Lacks, D. J., & Levandovsky, A. 2007, J. Electrostat., 65, 107
Lamb, D., & Verlinde, J. 2011, Physics and Chemistry of Clouds (Cambridge: Cambridge Univ. Press)
MacGorman, D. R., & Rust, W. D. 1998, The Electric Nature of Storm (Oxford: Oxford Univ. Press)
Marshall, T. C., Rison, W. D., Rust, M., et al. 1995, JGR, 100, 20815
Marshall, T. C., Stolzenburg, M., Maggio, C. R., & Coleman, L. M. 2005, GeoRL, 32, L03813
Meek, J. M., & Craggs, J. D. 1978, Electrical Breakdown of Gases (New York: Wiley)
Merrison, J. P., Gunnlaugsson, H. P., Hogg, M. R., et al. 2012, P&SS, 60, 328
Michael, M., Tripathi, S. N., & Mishra, S. K. 2008, JGR, 113, 7010
Pähtz, T., Herrman, H. J., & Shinbrot, T. 2010, NatPh, 6, 374
Pont, F., Knutson, H., Gilliland, R. L., Moutou, C., & Charbonneau, D. 2008, MNRAS, 385, 109
Poppe, T., Blum, J., & Henning, T. 2000, ApJ, 533, 472
Raether, H. 1964, Electron Avalanches and Break Down in Gases (London: Butterworths)
Raizer, Y. P. 1991, Gas Discharge Physics (Berlin: Springer)
Roussel-Dupre, R., Colman, J. J., Symbalisty, E., Sentman, D., & Paski, V. P. 2008, SSRv, 137, 51
Saunders, R. W., & Plane, J. M. C. 2011, Icar, 212, 373
Scholz, A., Irwin, J., Bouvier, J., Sipöcz, B. M., & Hodgkin, S. 2011, MNRAS, 413, 259
Sentman, D. D. 2004, in ISUAL Workshop Proc., Electrical Breakdown Parameters for Neutral Atmospheres of the Solar System, 08-013-0016
Sickafoose, A. A., Colwell, J. E., Horany, M., & Robertson, S. 2000, PhRvL, 84, 6034
Sing, D. K., Desert, J.-M., Lecavelier Des Etangs, A., et al. 2009, A&A, 505, 891
Sing, D. K., Pont, F., Aigrain, S., et al. 2011, MNRAS, 416, 1443
Stark, C. R., Potts, H. E., & Diver, D. A. 2006, A&A, 457, 365
Witte, S., Helling, Ch., Barman, T., Heidrich, N., & Hauschildt, P. H. 2011, A&A, 529, 44
Witte, S., Helling, Ch., & Hauschildt, P. H. 2009, A&A, 506, 1367
Woitke, P., & Helling, Ch. 2003, A&A, 399, 297
Woitke, P., & Helling, Ch. 2004, A&A, 423, 657
Yair, Y., Levin, A., & Tzivion, S. 1995, Icar, 115, 421
Yuan, T., Remer, L. A., Pickering, K. E., & Yu, H. 2011, GeoRL, 38, 4701